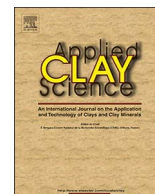




Contents lists available at ScienceDirect

Applied Clay Science

journal homepage: [www.elsevier.com/locate/clay](http://www.elsevier.com/locate/clay)

Research paper

# Influence of formulation on morphology and rheology of polypropylene/polyamide blends filled with nanoclay mineral particles

Quentin Beuguel, Julien Ville, Jérôme Crepin-Leblond, Pascal Mederic, Thierry Aubry\*

IRDL – FRE CNRS-3744, Université de Bretagne Occidentale – UFR Sciences et Techniques, 6 avenue Victor le Gorgeu – CS 93 837, 29 238 Brest Cedex 3, France

## ARTICLE INFO

### Keywords:

Polypropylene/polyamide blends  
Synthetic talc  
Montmorillonite  
Interphase  
Viscoelasticity  
Morphology

## ABSTRACT

The effect of formulation on the morphological and rheological properties of clay polypropylene/polyamide 12 nanocomposites is investigated. Two clay minerals, organically modified montmorillonite and synthetic talc, and two polypropylenes matrices, a low viscosity polypropylene and a high viscosity polypropylene, are used. The higher polypropylene matrix viscosity strongly influences the interfacial coverage of polyamide nodules, by slowing down the migration of fillers from polypropylene matrix to polyamide nodules. The nature of clay minerals as well as the polypropylene matrix viscosity is shown to influence the change from nodular to non-nodular morphology of nanocomposites. A comparative study of the viscoelastic properties of montmorillonite or synthetic talc high viscosity polypropylene/polyamide 12 nanocomposites is performed through the use of Palierne's model. Surprisingly, the results show that a developed montmorillonite interphase behaves like a weakly developed synthetic talc interphase suggesting that the nature and structure of clay particles located at the interface play a key role in interphase viscoelastic properties.

## 1. Introduction

Over the past decades, immiscible thermoplastic blends have been widely used because of their improved properties, as compared to those of the neat thermoplastics. Polypropylene/polyamide (PP/PA) blends are commonly used in industrial applications, because these two polymers are cheap, complementary and easily processed. For example, barrier properties to hydrocarbon or impact strength of polypropylene matrix were shown to be enhanced by addition of a polyamide dispersed phase (Utracki, 1998). The blend morphology, either nodular, fibrillar, lamellar or co-continuous, depends on thermomechanical conditions imposed during mixing, on viscoelastic properties of both components (Starita, 1972; Grace, 1982) and on the dispersed phase fraction (Huitric et al., 1998).

In order to obtain a fine dispersion, to stabilize the morphology and to enhance interfacial adhesion, the most efficient strategy is to add a macromolecular compatibilizer (Utracki, 1991; Moan et al., 2000). However, it was recognized that addition of small amounts of nanoparticles was a promising alternative route to compatibilize immiscible polymer blends. In particular, plate-like nanoparticles were shown to be effective in promoting refinement of the blend morphology (Salzano de Luna and Filippone, 2016), resulting in an improvement of end-use properties (Mehrabzadeh and Kamal, 2002; Gelfer et al., 2003; Wang et al., 2003; Ray et al., 2006; Brulé and Flat, 2006; Yousfi et al., 2014;

Motamedi and Bagheri, 2016; Huitric et al., 2017). However, The compatibilizing effect was clearly shown to be strongly influenced by the location of nanoparticles within polymer blends, which depends on structural characteristics of fillers (Médéric et al., 2011), on specific affinity of nanoparticles towards polymer phases (Sumita et al., 1991; Steimann et al., 2002; Beuguel et al., 2017) and on rheological properties of both polymer phases (Feng et al., 2003; Labaume et al., 2013a).

Among plate-like nanoparticles, organically modified montmorillonite (Mt) nanolayers are most commonly incorporated into polypropylene/polyamide blends. Firstly, Mt selective affinity towards polar thermoplastics favors their intercalation by PA chains, leading to a high degree of exfoliation (Aubry et al., 2005). Secondly, it was shown that Mt nanoparticles can easily migrate to the interface of the two thermoplastic phases, leading to the formation of an interphase, with numerous structural defects (Labaume et al., 2013b). The interphase inhibits dispersed phase droplet coalescence through steric repulsion (Gahleitner et al., 2006; Ville et al., 2012), but destabilizes the nodular morphology at a weak Mt volume fraction, ~1% (Labaume et al., 2013a; Huang et al., 2014; Beuguel et al., 2017). More recently, synthetic talc (ST) nanolayers, provided under the hydrogel form (Martin et al., 2008a, b, c; Leroux et al., 2013), have shown their efficiency to reduce dispersed phase nodule size. More precisely, ST particles, exclusively located within dispersed PA phase and exhibiting numerous

\* Corresponding author.

E-mail address: [thierry.aubry@univ-brest.fr](mailto:thierry.aubry@univ-brest.fr) (T. Aubry).

<http://dx.doi.org/10.1016/j.clay.2017.07.031>

Received 27 March 2017; Received in revised form 30 June 2017; Accepted 26 July 2017  
0169-1317/ © 2017 Published by Elsevier B.V.

stacking defects (Dumas et al., 2013), were shown to be weakness sites favoring the nodule break-up (Beuguel et al., 2017).

Rheology is a powerful tool to characterize the effect of a compatibilizer added to an immiscible polymer blend. For example, oscillatory shear rheometrical tests, performed on blends compatibilized with nanoparticles (Labaume et al., 2013b), have highlighted the existence of two relaxation times: a nodule form relaxation time and a longer characteristic time attributed to the relaxation of a sufficiently developed interphase. From a modeling point of view, the Palierné's model (Palierné, 1990) with a non-isotropic frequency and strain dependent interfacial stress tensor, was required to correctly describe the viscoelastic behavior of immiscible polymer blends exhibiting droplet morphology with fully developed interphase (Labaume et al., 2013b). In the case of weakly compatibilized blends, the simplified version of Palierné's model has been successfully used to describe the viscoelastic properties (Fenouillot et al., 2009).

The aim of the present work was to study some formulation effects on the morphological and rheological properties of clay PP/PA12 nanocomposites, focusing on the effect of PP matrix viscosity and clay mineral nature (Mt or ST). A particular attention was paid to the effect of PP matrix viscosity on the viscoelastic properties of the interphase, through the use of Palierné's model.

## 2. Materials and methods

### 2.1. Materials

Blends were prepared using two matrices: a low viscosity polypropylene (LVPP) and a high viscosity polypropylene (HVPP), supplied by Lyondellbasell (Moplen® HP500N) and Bolloré (PPR®), respectively. The dispersed phase is a commercial polyamide 12 (PA12), supplied by Arkema (Rilsan® AECHVO). The specific gravity, the melting point,  $T_m$ , and the Newtonian viscosity,  $\eta_0^*$ , measured at 220 °C, of LVPP, HVPP and PA12 are reported in Table 1.

The viscosity ratio, defined as the ratio of the Newtonian viscosity of the dispersed phase to that of the matrix, is  $\sim 0.8$  for the LVPP/PA12 blend and  $\sim 0.1$  for the HVPP/PA12 blend. Viscosity measurements, performed on a RT 1000 Göttfert capillary rheometer, have shown that viscosity ratios were not significantly changed at higher shear rates encountered during melt mixing (Beuguel et al., 2017).

The organically modified montmorillonite, named Cloisite 30B®, is supplied by Southern Clay Products. It is a methyl tallow bis-2-hydroxyethyls ammonium exchanged montmorillonite, with a modifier concentration of 90 milliequivalent per 100 g. This organophilic Mt has a good affinity towards polyamide 12 (Aubry et al., 2005), but a very poor affinity towards an apolar phase (Médéric et al., 2005), like PP. The individual Mt layer is  $\sim 0.7$  nm thick and  $\sim 200$  nm long (Paul and Robeson, 2008). For Mt particles, the interlayer distance, corresponding to basal distance (d001) as estimated from XRD measurements, using Bragg's equation, is close to 1.2 nm. The specific gravity of Mt is close to 2.

The synthetic talc (ST) hydrogel was prepared by GET laboratory (University Paul Sabatier, France), according to a patented hydrothermal process (Le Roux et al., 2013). ST nanoparticles have a higher affinity towards PA than towards PP, due to strong polar-polar interactions (Yousfi et al., 2014). The ST particle average length and

**Table 1**  
Characteristics of LVPP, HVPP and PA12 phases.

	LVPP	HVPP	PA12
Specific gravity	0.9	0.9	1.01
$T_m$ (°C)	165	165	183
$\eta_0^*$ (Pa·s) at 220 °C	580	4000	450

thickness are about 150 nm (Dumas et al., 2013) and 8 nm (Beuguel et al., 2015), respectively. The basal distance is 0.3 nm. The specific gravity of ST is  $\sim 2.8$ .

### 2.2. Sample preparation

Because of the hygroscopic character of PA12, all samples were dried in vacuum at 80 °C during 4 h. All components were simultaneously melt mixed for 6 min, at 220 °C and 50 rpm, using DSM Xplore lab twin screw extruder. Then, the samples were pelletized and compression molded into 1.5 mm thick plates using a Darragon hot press. During compression, the temperature was fixed at 220 °C, and the pressure was increased by steps, from 0 to 25 MPa in order to avoid the formation of air bubbles. All samples have been prepared at a PA12 dispersed phase mass fraction of 20%, which is expected to lead to a nodular morphology (Huitric et al., 2009; Ville et al., 2012). The filler volume fraction,  $\phi$  ranges from 0.3% to 1% for Mt and from 0.4% to 5.8% for ST, relative to PA.

### 2.3. Structural and morphological characterizations

The morphology of all samples was investigated from the observation of a vacuum-metallized surface of cryofractured samples, by using a Hitachi S-3200N Scanning Electron Microscopy (SEM), with an accelerating voltage of 15 kV. The volume and number average diameters,  $D_v$  and  $D_n$ , were determined from SEM micrographs by measuring at least 200 PA nodules with SigmaScan® PRO 5.0 image analysis software; the ratio  $D_v/D_n$  defines the polydispersity index.

The location of nanoparticles was observed using JEOL 1400 Transmission Electron Microscope (TEM) at 100 kV. Samples were prepared at  $-130$  °C with an ultracryomicrotome (Reichert Jung), equipped with a diamond knife, in order to obtain 40 nm thick ultrathin sections. In case clay particles are located at the interface, the average interphase thickness and the interfacial coverage were measured, as performed in previous works (Huitric et al., 2009; Ville et al., 2012). The average length,  $L$ , and thickness,  $e$ , of clay mineral particles located within PA nodules, as well as the specific particle density,  $d_{sp}$ , that is the number of particles dispersed per  $\mu\text{m}^2$  of PA divided by the filler mass fraction (Fornès et al., 2001), were estimated.

### 2.4. Rheometrical measurements

Oscillatory shear tests were performed using a controlled strain rheometer (Gemini) equipped with parallel plate geometry (25 mm diameter and 1.5 mm spacing). All viscoelastic measurements were carried out at 200 °C, under a continuous purge of dry nitrogen in order to avoid sample degradation. All frequency sweep tests were performed at a strain amplitude of 4%, which lies in the linear viscoelastic regime for all samples tested. No time evolution of rheological data was observed over 30 min. All rheometrical experiments obtained within 20 min were shown to be reproducible within  $\pm 5\%$ .

Weighted relaxation spectra  $\lambda H(\lambda)$  have been calculated from storage modulus  $G'$  and loss modulus  $G''$  versus frequency measurements, using a nonlinear regularization method (Honerkamp and Weese, 1993).

### 2.5. Rheological modeling

Palierné's model is an emulsion model of viscoelastic fluids. The interfacial stress tensor  $\underline{\alpha}$  is assumed to be decomposed into an isotropic interfacial tension,  $\alpha \underline{\delta}$  ( $\underline{\delta}$  is the unit tensor), and a non-isotropic part,  $\underline{\beta}$ , depending on the frequency  $\omega$  and the strain tensor  $\underline{\gamma}$ :

$$\underline{\alpha} = \alpha \underline{\delta} + \underline{\beta} = \alpha \underline{\delta} + \frac{1}{2} \beta_d^*(\omega) (\text{tr}(\underline{\gamma})) \underline{\delta} + \beta_s^*(\omega) \left( \underline{\gamma} - \frac{1}{2} (\text{tr}(\underline{\gamma})) \underline{\delta} \right) \quad (1)$$

where  $\text{tr}$  is the trace of the strain tensor  $\underline{\gamma}$ .  $\beta_d^*(\omega)$  and  $\beta_s^*(\omega)$  are defined

Download English Version:

<https://daneshyari.com/en/article/5468582>

Download Persian Version:

<https://daneshyari.com/article/5468582>

[Daneshyari.com](https://daneshyari.com)